Peer-reviewed version available at *Sensors* **2018**, *18*, 4304; doi:10.3390/s18124304

Article

Highly Sensitive Detection of 4-Methylimidazole Using a Terahertz Metamaterial

Hee Jun Shin[1], Hae Won Jang[2], Gyeongsik Ok[3,*]

[1] Pohang Accelerator Laboratory, 80 Jigokro-127-beongil, Nam-Gu, Pohang, Gyeongbuk, 37673, Republic of Korea
[2] Research Group of Food Processing, Korea Food Research Institute, 245, Nongsaengmyeong-ro, Iseo-myeon, Wanju-gun, Jeollabuk-do 55365, Republic of Korea
[3] Research Group of Consumer Safety, Korea Food Research Institute, 245, Nongsaengmyeong-ro, Iseo-myeon, Wanju-gun, Jeollabuk-do 55365, Republic of Korea

* Correspondence: gsok@kfri.re.kr; Tel.: +82-63-219-9408

Abstract: We demonstrate, for the first time, a highly sensitive detection of 4-methylimidazole (4-MeI), a carcinogenic material, by applying an electric field enhancement technique using a terahertz (THz) metamaterial at the THz region. The THz metamaterials were fabricated with a metal array using an electric-field-coupled inductor-capacitor (ELC) resonator structure, and FDTD simulation showed good agreement with experimental results. We measured the THz spectra of the metamaterials to detect 4-MeI concentrations of 0, 1, 2, 5, 10, 15, and 20 mg/L. The resonance frequency of the metamaterial was shifted by approximately 8 GHz and transmittance at the resonance frequency increased to 2 x 10-3 as the concentration was increased, up to 20 mg/L. Our study provides new insight into application of metamaterials to detect carcinogen using a THz technique.

Keywords: THz spectroscopy; 4-methylimidazole; metamaterial; carcinogen detection

1. Introduction

Several soft drinks including sodas, energy drinks, and diet drinks contain caramel color which is widely used as a coloring and flavoring agent [1,2]. Caramel colored drinks including colas, root beer, and black tea are widely consumed across the world in large amounts. However, caramel color agents have attracted significant attention because it was found that caramel colored drinks may contain 4-methylimidazole (4-MeI), which is known to be carcinogenic [1, 3-5]. Caramel colors are usually classified into four types, Caramel I, II, III, and IV, and their production and choice of reagents are based on their applications [2,3]. The compound 4-MeI is formed during the production of caramel colors type III and IV, which contain ammonium compounds. Detecting 4-MeI in food products has been an ongoing challenge, with several studies directed at developing efficient methods. For example, high performance liquid chromatography (HPLC) [6], HPLC-mass spectroscopy [3,7], gas chromatography (GC) [8] and GC-mass spectroscopy [9,10] have been used to detect 4-MeI, in addition to 2-dimensional liquid chromatography [11,12]. Spectral properties of various imidazole compounds and characteristics of imidazole isomers can be investigated using nuclear magnetic resonance and mass spectroscopy [13,14]. However, new detection techniques using label-free technologies with high sensitivity and ease of use have been in high demand, especially in cases of chemical or biological material testing.

Following recent reports that terahertz (THz) waves can be generated using a femtosecond laser, application of the THz frequency range has gained significant attention in various research areas including biochemistry [15-18], electronics [19], photonics [20,21], astronomy [22], military science [23], food science

[24,25], and medical diagnosis [26,27]. In particular, THz techniques such as THz time-domain spectroscopy have emerged as attractive techniques that can enable label free, non-contact, and non-destructive detection in biological and chemical materials [18,28,29]. The THz range can reveal several types of information in biological and chemical materials; for example, various conformational energies such as rotation, vibration, and intermolecular interactions of chemical and biological molecules occur in the THz range [18,24,30]. Recent efforts to improve sensitivity of biochemical detection have involved the use of various artificial structures fabricated using metamaterials. Metamaterials have several significant advantages including easy preparation, easy handling, high sensitivity, and material-selective procedures. Usually, artificial structures created using conductive materials such as metals are used for patterning metamaterials, and this provides an opportunity to control electromagnetic properties and functionalities of the materials. In addition, metamaterials have been designed to function in various frequency ranges using their unique properties including negative refractive index, and high absorbance at specific frequencies. In particular, THz metamaterials have been widely studied because they can be used to design artificial structures to enhance detection of several chemical and biological materials in the THz range. THz metamaterials can be used to markedly enhance biochemical molecular energies in the THz region, and they have been investigated in various biological and chemical studies [31-35].

In the present study, we demonstrate detection of 4-MeI, a possible carcinogenic component in caramel colored drinks, using THz metamaterials for the first time. We measured the THz spectrum of 4-MeI in the frequency range from 0.2 to 2 THz using THz transmission mode spectroscopy. Using a THz metamaterial at the resonance frequency of 4-MeI, we investigated its frequency shift enhancement for 4-MeI detection.

2. Materials and Experiment

2.1 Metamaterial fabrication

The THz metamaterial was fabricated using an electric-field-coupled inductor-capacitor (ELC) resonator structure [36,37]. The metamaterial was based on a metallic array consisting of a square ring with a micro split gap structure. A polyimide (PI) solution was spin coated on the Si wafer at a thickness of 500 μm at 2500 rpm. The Si wafer with coated PI solution was baked at 110 °C for three minutes. To deposit an Au pattern on the PI/Si wafer, we adopted a lift-off process. The PI/Si wafer substrate was photoresist coated at 3000 rpm for 40 seconds and soft baked at 95 °C for 90 seconds. Next, the substrate was exposed to UV for three seconds. Hard baking was performed at 110 °C for three minutes followed again by UV exposure for 30 seconds. Finally, the photoresist was developed. We deposited a Ti 30 nm / Au 100 nm layer on the PI/Si wafer. The schematic of the metamaterial is shown in Fig. 1(a). We simulated metamaterial design using a finite-difference time-domain (FDTD) method in the terahertz range.

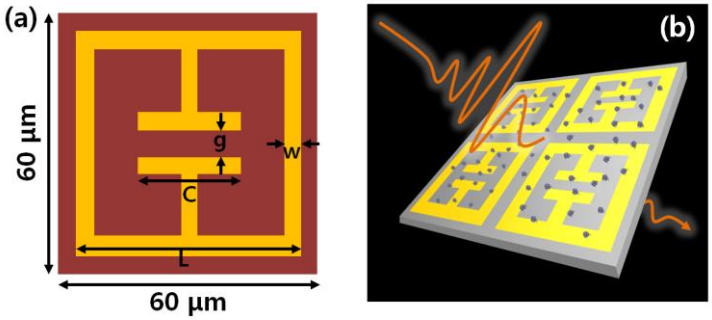

Figure 1. Schematic of (a) the THz metamaterial and (b) THz measurement using the metamaterial.

Preprints (www.preprints.org) | NOT PEER-REVIEWED | Posted: 18 October 2018 doi:10.20944/preprints201810.0421.v1

Peer-reviewed version available at Sensors 2018, 18, 4304; doi:10.3390/s18124304

As can be seen in Fig. 1(b), a THz electric field passing through the metamaterial is scattered by 4-MeI molecules in a vertical direction. The THz output signal throughout the metamaterial was analyzed using a Fourier transformation-based method. A commercial THz time-domain spectroscopy system (TPS-3000, Teraview, UK) was used to obtain THz spectra of the pellet sample and the metamaterial in the frequency range from 0.2 to 2 THz. All of the experimental THz-TDS measurements were performed at room temperature and the humidity in the THz-TDS system was maintained lower than 1 % using dried air during THz spectra measurement of the samples.

The output THz signal $O(\omega)$ passing through a sample is related to the input signal $I(\omega)$ as follows [18]

$$O(\omega) = I(\omega)\exp\left[-\frac{d\alpha(\omega)}{2}\right]\exp\left[i\frac{2\pi}{\lambda}n_1(\omega)d\right], \quad (1)$$

where $I(\omega)$ is the complex input signal, $\alpha(\omega)$ is the absorption coefficient, d is the thickness of the sample, λ is the wavelength, and n is the refractive index of the sample. Power absorption can be obtained from the difference between spectral amplitudes with and without the sample.

$$\alpha(\omega) = -\frac{2}{d}ln\left[\frac{O(\omega)}{I(\omega)}\right]. \quad (2)$$

2.2 4-MeI sample preparation

A commercially available 4-MeI product was obtained (Sigma-Aldrich, US). We crushed the dry 4-MeI into small particles less than the THz wavelength to prevent scattering. To measure the THz spectrum, the 4-MeI (30 mg) was prepared as pellet sample compounded with polyethylene (PE) powder (270 mg). In addition, we prepared 4-MeI solutions to apply onto the THz metamaterial at concentrations of 0, 1, 2, 5, 10, 15 and 20 mg/L of 4-MeI in distilled water. 10 μL of the 4-MeI solutions at each concentration were dropped onto the THz metamaterial and dried at 70 °C for 10 min until the water evaporated completely. Next, the THz metamaterial was cooled at room temperature for 30 min to maintain identical conditions for each measurement. A schematic of the process is shown in Fig. 2.

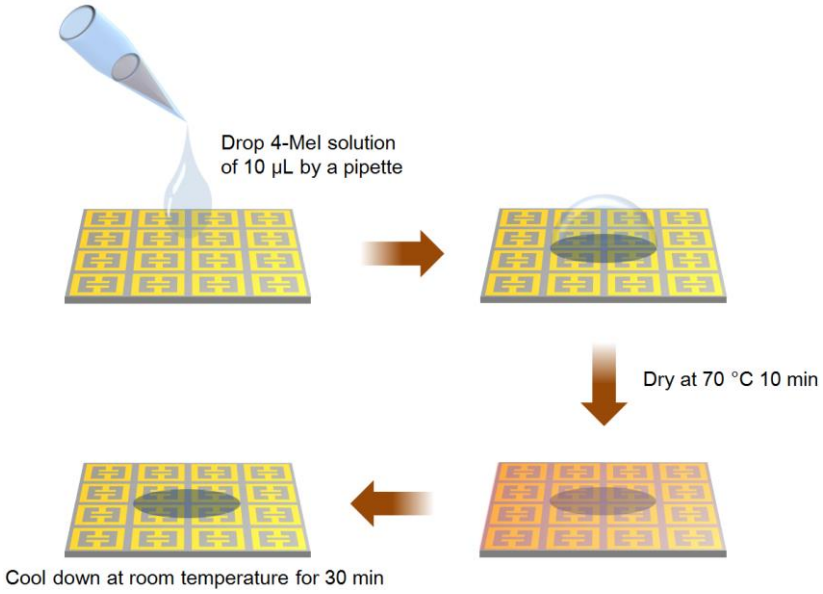

Figure 2. Schematic of drop coating deposition of the 4-MeI sample on the THz metamaterial.

Preprints (www.preprints.org) | NOT PEER-REVIEWED | Posted: 18 October 2018 doi:10.20944/preprints201810.0421.v1

Peer-reviewed version available at Sensors 2018, 18, 4304; doi:10.3390/s18124304

3. Results and Discussion

3.1 THz spectrum of a 4-MeI pellet

We first describe the THz spectral characteristics of 4-MeI using THz-TDS. We measured THz spectra of a pellet composed of PE and 4-MeI, and the spectra are shown in Fig. 3. As can be seen in the figure, the PE pellet showed a low absorption and had no resonance peak at the measured THz region. From the THz spectrum of the PE pellet, we obtained the THz spectrum of 4-MeI by extracting the absorbance of PE. The spectrum of the pellet composed of PE and 4-MeI showed the two significant 4-MeI resonance peaks at 0.56 and 0.82 THz. In particular, the spectrum of 4-MeI shows a more intense absorption peak at 0.82 THz than at 0.56 THz.

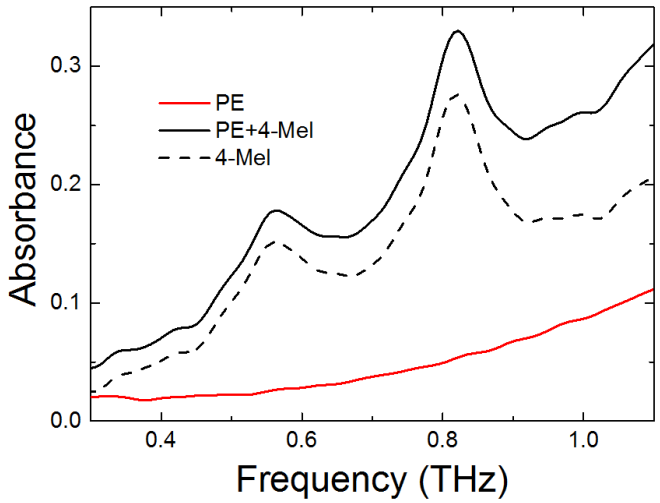

Figure 3. The spectra of polyethylene and 4-methylimidazole pellets at the THz region from 0.2 to 1.1 THz.

3.2 4-MeI detection in the THz metamaterial

To fabricate frequency-selective metamaterials for 4-MeI, as shown in Fig. 1, the metamaterial was designed to encompass a resonance frequency of 0.82 THz which is the resonance frequency of 4-MeI. The resonant peak position of the transmittance was determined based on the capacitor length and the gap of the metamaterial [31]. The capacitor length (C) and the gap (g) were designed to be 20 μm and 8 μm. The full length (L) of the metamaterial was 54 μm as shown in Fig. 1(a). The simulation and experimental results are shown in Fig. 4(a). The normalized THz spectrum of the metamaterial illustrates a resonant feature at 0.82 THz. As can be seen in Fig. 4(a), the experimental spectrum of the THz metamaterial is in good agreement with the FDTD simulation. In addition, at the resonance frequency, we found that the localized THz electric field is strongly enhanced at the gap of the antenna in the simulation as shown in the inset in Fig. 4(a). Fig. 4(b) shows a scanning optical microscope image of the fabricated THz metamaterial. When the 4-MeI sample is dropped on the THz metamaterial, the 4-MeI molecules significantly interact with the localized strong THz field and the features of the metamaterial changes as the 4-MeI concentration increases. Consequently, the resonant peak position and/or the transmittance are changed.

Preprints (www.preprints.org) | NOT PEER-REVIEWED | Posted: 18 October 2018 doi:10.20944/preprints201810.0421.v1

Peer-reviewed version available at Sensors 2018, 18, 4304; doi:10.3390/s18124304

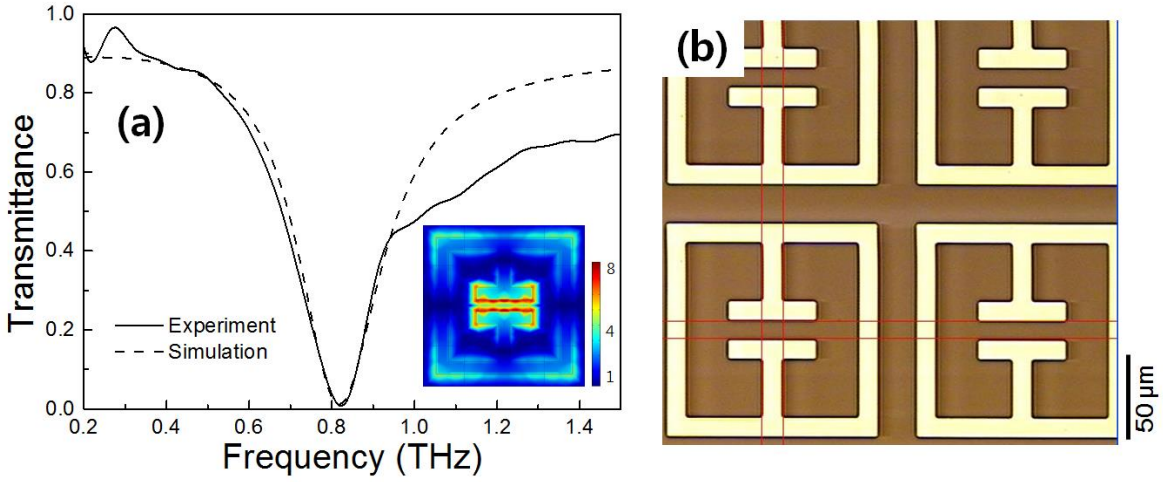

Figure 4. (a) Transmittance curves obtained in the experiment and the simulation using the THz metamaterial. (b) Optical microscope image of the THz metamaterial.

Fig. 5 illustrates the full THz spectra of the metamaterial at different 4-MeI concentrations of 0, 1, 2, 5, 10, 15, and 20 mg/L. The inset in Fig. 5 shows a zoomed-in image of the resonant region. As seen in the figure, the resonant peak of the THz metamaterial shifts to a lower frequency as the 4-MeI concentration increases. In addition, the transmittance also increases slightly. The 4-MeI concentration-dependence of the resonance frequency and the transmittance of the THz metamaterial is shown in Fig. 6. In Fig. 6(a), the resonance frequency is shifted to a lower frequency as the concentration of 4-MeI increases. In addition, the transmittance increases as the concentration of 4-MeI increases. The behavior of the resonance frequency and the transmittance can be explained by fitting to a linear equation. The resonance frequency shift fits to the linear equation $Y= -0.31X+820.56$ and the transmittance change fits to $Y=8.1\times10^{-3}X+7.8\times10^{3}$ with increasing 4-MeI concentration. As a result, the resonance frequency is shifted by approximately 8 GHz and the transmittance at the resonance frequency increases to 2×10^{-3} as the concentration increases to 20 mg/L. These results indicate that a few mg/L of 4-MeI present in food material such as a beverage, can be detected using this metamaterial. However, the sensitivity of the metamaterial needs to be improved by using a higher sharp resonant peak or enhancing interactions between over-layered materials and an electric field near the metal structure, which would enable detection of 4-MeI of less than a few hundred mg/L.

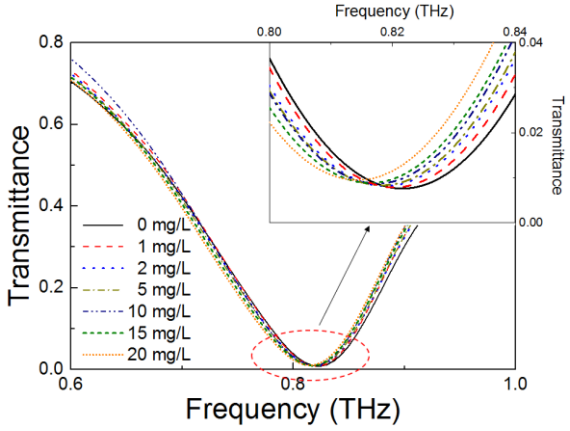

Figure 5. Spectra of 4-MeI detection using the THz metamaterial at concentrations of 0, 1, 2, 5, 10, 15, and 20 mg/L in the THz region from 0.6 to 1.0 THz.

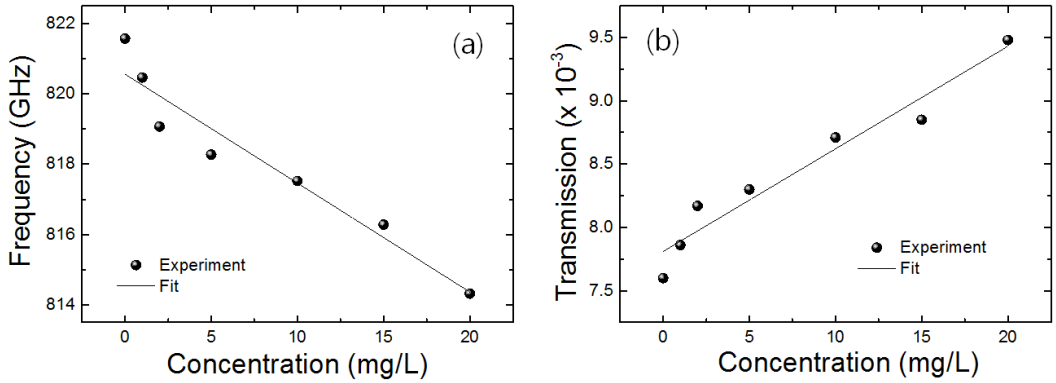

Figure 6. (a) The resonance frequency and (b) transmittance of the THz metamaterial as the concentration of 4-MeI increases. Solid lines indicate linear fits of the experimental results.

The present study provides experimental evidence supporting the fact that the application of metamaterials combined with THz technology has substantial potential in detection of hazardous materials in food products. Further studies may involve fabrication of THz metamaterials with sharp resonant peaks and high sensitivity with a nano-slit structure, to improve the sensitivity of the metamaterials in detecting 4-MeI as well as other carcinogenic substances.

4. Conclusions

In conclusion, we report, for the first time, a THz metamaterial-based detection of the carcinogenic substance 4-MeI which may be present in caramel colored food products. We measured THz spectra of pellets containing 4-MeI and PE and observed resonance peaks at 0.56 and 0.82 THz. We fabricated a THz metamaterial with a resonance feature at 0.82 THz and measured THz spectra at 4-MeI concentrations ranging from 0 to 20 mg/L. We found that the resonance frequency decreases and the transmittance increases as the 4-MeI concentration increases. We were able to clearly detect 4-MeI using the THz metamaterial and the results demonstrate highly sensitive detection. Thus, our findings provide new insight into 4-MeI detection and potential applications of metamaterials-based technology in food safety inspection.

Acknowledgments: This work was supported financially by Main Research Program of the Korea Food Research Institute funded by the Ministry of Science, ICT & Future Planning (E0187801-01).

Author Contributions: Gyeongsik Ok and Hee Jun Shin conceived and designed concept of the experiments. Hee Jun Shin wrote the manuscript and analyzed the experimental results. 4-methylimidazole samples were prepared by Hae Won Jang. THz time-domain spectroscopy characteristics of 4-methylimidazole and metamaterials were carried out by Hee Jun Shin. All the authors participated in discussion and the results.

Conflicts of Interest: The authors declare no conflict of interest.

References

[1] Lee, K. G.; Jang, H.; Shibamoto, T. Formation of carcinogenic 4(5)-methylimidazole in caramel model systems: A role of sulphite. *Food Chem*., **2013,** 136, 1165-1168, https://doi.org/10.1016/j.foodchem.2012.09.025.

[2] Chappel, C. I.; Howell, J. C. Caramel colours–A historical introduction. *Food Chem. Toxicol*., **1992,** 30, 351–357, https://doi.org/10.1016/0278-6915(92)90060-X.

[3] Yamaguchi, H.; Masuda, T. Determination of 4-MI in soy sauce and other foods by LC-MS after solid-phase extraction. *J. Agric. Food Chem*., **2011**, 59, 9770–9775, DOI: 10.1021/jf201736c.

[4] Hengel, M.; Shibamoto, T. Carcinogenic 4 (5)-methylimidazole found in beverages, sauces, and caramel colors: chemical properties, analysis, and biological activities. *J. Agric. Food Chem*., **2013**, 61(4), 780-789, DOI: 10.1021/jf304855u.

[5] Moon, J. K.; Shibamoto, T. Formation of carcinogenic 4 (5)-methylimidazole in Maillard reaction systems. *J. Agric. Food Chem*., **2010**, 59(2), 615-618, DOI: 10.1021/jf104098a.

[6] Lawrence, J. F.; Charbonneau, C. F. Direct method for the determination of 2-acetyl-4 (5)-tetrahydroxy-butylimidazole in caramel colours and beers by high-performance liquid chromatography. *J. Chromatogr. A*, **1987**, 407, 405-407, https://doi.org/10.1016/S0021-9673(01)92645-7.

[7] Klejdus, B.; Moravcová, J.; Kubáň, V. Reversed-phase high-performance liquid chromatographic/mass spectrometric method for separation of 4-methylimidazole and 2-acetyl-4-(1, 2, 3, 4-tetrahydroxybutyl) imidazole at pg levels. *Anal. Chim. Acta*, **2003**, 477(1), 49-58, https://doi.org/10.1016/S0003-2670(02)01409-5.

[8] Cerny, M.;Blumenthal, A. 4-Methylimidazol in Caramel und caramelgefärbten Lebensmitteln. *Z. Lebensm. Unters. Forsch. A*, **1979**, 168(2), 87-90, https://doi.org/10.1007/BF01127510.

[9] Fuchs, G.; Sundell, S. Quantitative determination of 4-methylimidazole as 1-acetyl derivative in caramel color by gas-liquid chromatography. *J. Agric. Food Chem*., **1975**, 23(1), 120-122, https://pubs.acs.org/doi/pdf/10.1021/jf60197a013.

[10] Pons, I.; Garrault, C.; Jaubert, J. N.; Morel, J.; Fenyo, J. C. Analysis of aromatic caramel. *Food Chem.*, **1991**, 39(3), 311-320, https://doi.org/10.1016/0308-8146(91)90148-H.

[11] Liu, J.; Sun, J.; Sui, X.; Wang, Y.; Hou, Y.; He, Z. Predicting blood–brain barrier penetration of drugs by microemulsion liquid chromatography with corrected retention factor. *J. Chromatogr. A*, **2008**, 1198, 164-172, https://doi.org/10.1016/j.chroma.2008.05.065.

[12] Moretton, C.; Crétier, G.; Nigay, H.; Rocca, J. L. Quantification of 4-methylimidazole in class III and IV caramel colors: validation of a new method based on heart-cutting two-dimensional liquid chromatography (LC-LC). *J. Agric. Food Chem.*, **2011**, 59(8), 3544-3550, DOI: 10.1021/jf104464f.

[13] Matthews, H. R.; Rapoport, H. Differentiation of 1, 4-and 1, 5-disubstituted imidazoles. *J. Am. Chem. Soc.*, **1973**, 95(7), 2297-2303, https://pubs.acs.org/doi/pdf/10.1021/ja00788a033.

[14] Bowie, J. H.; Cooks, R. G.; Lawesson, S.; Schroll, G. Electron impact studies. XII. Mass spectra of substituted imidazoles. *Aust. J. Chem.*, **1967**, 20(8), 1613-1624, https://doi.org/10.1071/CH9671613.

[15] Smye, S. W.; Chamberlain, J. M.; Fitzgerald, A. J.; Berry, E. The interaction between terahertz radiation and biological tissue. *Physics in Medicine & Biology*, **2001**, 46(9), R101, http://iopscience.iop.org/article/10.1088/0031-9155/46/9/201/pdf.

[16] Upadhya, P. C.; Shen, Y. C.; Davies, A. G.; Linfield, E. H. Terahertz time-domain spectroscopy of glucose and uric acid. *Journal of Biological Physics*, **2003**, 29(2-3), 117-121, https://doi.org/10.1023/A:1024476322147.

[17] Ajito, K.; Ueno, Y. THz chemical imaging for biological applications. *IEEE Transactions on Terahertz Science and Technology*, **2011**, 1(1), 293-300, DOI: 10.1109/TTHZ.2011.2159562.

[18] Shin, H. J.; Oh, S. J.; Kim, S. I.; Won Kim, H.; Son, J. H. Conformational characteristics of β-glucan in laminarin probed by terahertz spectroscopy. *Appl. Phys. Lett.*, **2009**, 94(11), 111911, https://doi.org/10.1063/1.3100778.

[19] Otsuji, T., Popov, V.; Ryzhii, V. Active graphene plasmonics for terahertz device applications. *Journal of Physics D: Applied Physics*, **2014**, 47(9), 094006, http://iopscience.iop.org/article/10.1088/0022-

3727/47/9/094006/pdf.

[20] Shin, H. J.; Kim, J.; Kim, S.; Choi, H.; Lee, S.; Lee, Y. H.; Son, J, H.; Lim, S. C. Unsaturated drift velocity of monolayer graphene. *Nano letters*, **2018**, 18(3), 1575-1581, DOI: 10.1021/acs.nanolett.7b03566.

[21] Shin, H. J.; Kim, S. H.; Park, K.; Lim, M. C.; Choi, S. W.; Ok, G. Free-standing guided-mode resonance humidity sensor in terahertz. *Sensors and Actuators A: Physical*, **2017**, 268, 27-31, https://doi.org/10.1016/j.sna.2017.10.060.

[22] Mayorga, I. C.; Schmitz, A.; Klein, T.; Leinz, C.; Gusten, R. First in-field application of a full photonic local oscillator to terahertz astronomy. *IEEE Transactions on Terahertz Science and Technology*, **2012**, 2(4), 393-399, DOI: 10.1109/TTHZ.2012.2191286.

[23] Ergün, S.; Sönmez, S. Terahertz technology for military applications. *Journal of Military and Information Science*, **2015**, 3(1), 13-16, http://dergipark.gov.tr/download/article-file/177644.

[24] Shin, H. J.; Choi, S. W.; Ok, G. Qualitative identification of food materials by complex refractive index mapping in the terahertz range. *Food Chem.*, **2018**, 245, 282-288, https://doi.org/10.1016/j.foodchem.2017.10.056.

[25] Ok, G.; Park, K.; Lim, M. C.; Jang, H. J.; Choi, S. W. 140-GHz subwavelength transmission imaging for foreign body inspection in food products. *Journal of Food Engineering*, **2018**, 221, 124-131, https://doi.org/10.1016/j.jfoodeng.2017.10.011.

[26] Ji, Y. B.; Moon, I. S.; Bark, H. S.; Kim, S. H.; Park, D. W.; Noh, S. K.; Jeon, T. I. Terahertz otoscope and potential for diagnosing otitis media. *Biomedical Optics Express*, **2016**, 7(4), 1201, doi: 10.1364/BOE.7.001201.

[27] Oh, S. J.; Kim, S. H.; Ji, Y. B.; Jeong, K.; Park, Y.; Yang, J.; Park, D. W.; Noh, S. K.; Kang, S. G.; Huh, Y. M.; Son, J. H.; Suh, J. S. Study of freshly excised brain tissues using terahertz imaging. *Biomedical Optics Express*, **2014**, 5(8), 2837-2842, https://doi.org/10.1364/BOE.5.002837.

[28] Zhong, H.; Redo-Sanchez, A.; Zhang, X. C. Identification and classification of chemicals using terahertz reflective spectroscopic focal-plane imaging system. *Optics Express*, **2006**, 14(20), 9130-9141, https://doi.org/10.1364/OE.14.009130.

[29] Walther, M.; Fischer, B. M.; Ortner, A.; Bitzer, A.; Thoman, A.; Helm, H. Chemical sensing and imaging with pulsed terahertz radiation. *Analytical and Bioanalytical Chemistry*, **2010**, 397(3), 1009-1017, https://link.springer.com/content/pdf/10.1007%2Fs00216-010-3672-1.pdf.

[30] Rungsawang, R.; Ueno, Y.; Tomita, I.; Ajito, K. Terahertz notch filter using intermolecular hydrogen bonds in a sucrose crystal. *Opt. Express*, **2006**, 14(12), 5765-5772, ps://doi.org/10.1364/OE.14.005765.

[31] Park, S. J.; Hong, J. T.; Choi, S. J.; Kim, H. S.; Park, W. K.; Han, S. T.; Park, J. Y.; Lee, S.; Kim, D. S.; Ahn, Y. H. Detection of microorganisms using terahertz metamaterials. *Sci. Rep.*, **2014**, 4(4988), 1–7, https://doi.org/10.1038/srep04988.

[32] Reinhard, B.; Schmitt, K. M.; Wollrab, V.; Neu, J.; Beigang, R.; Rahm, M. Metamaterial near-field sensor for deep-subwavelength thickness measurements and sensitive refractometry in the terahertz frequency range. *Appl. Phys. Lett.*, **2012**, 100(22), 221101, https://doi.org/10.1063/1.4722801.

[33] Tao, H.; Strikwerda, A. C.; Liu, M.; Mondia, J. P.; Ekmekci, E.; Fan, K.; Kaplan, D. L.; Padilla, W. J.; Zhang, X.; Averitt, R. D.; Omenetto, F. G. Performance enhancement of terahertz metamaterials on ultrathin substrates for sensing applications. *Appl. Phys. Lett.*, **2010**, 97(26). 261909-261903, https://doi.org/10.1063/1.3533367.

[34] Xu, W.; Xie, L.; Zhu, J.; Wang, W.; Ye, Z.; Ma, Y.; Tsai, C. Y.; Chen, S.; Ying, Y. Terahertz sensing of chlorpyrifos-methyl using metamaterials. *Food Chem.*, **2017**, 218, 330-334, https://doi.org/10.1016/j.foodchem.2016.09.032.

[35] Qin, J.; Xie, L.; Ying, Y. A high-sensitivity terahertz spectroscopy technology for tetracycline hydrochloride detection using metamaterials. *Food Chem.*, **2016**, 211, 300-305, https://doi.org/10.1016/j.foodchem.2016.05.059.

[36] Schurig, D.; Mock, J. J.; Smith, D. R. Electric-field-coupled resonators for negative permittivity metamaterials. *Appl. Phys. Lett.*, **2016**, 88(4), 041109, https://doi.org/10.1063/1.2166681.

[37] Zhang, C. H.; Wu, J. B.; Jin, B. B.; Ji, Z. M.; Kang, L.; Xu, W. W.; Chen, J.; Tonouchi, M.; Wu, P. H. Low-loss terahertz metamaterial from superconducting niobium nitride films. *Opt. Express*, **2012**, 20(1), 42-47, https://doi.org/10.1364/OE.20.000042.